JOURNAL OF MATERIALS SCIENCE 23 (1988) 1967–1975

Impact response of short δ-alumina fibre/aluminium alloy metal matrix composites

C. M. FRIEND, A. C. NIXON
Materials Technology Group, Royal Military College of Science, Shrivenham, Swindon, Wiltshire SN6 8LA, UK

The impact response of pseudorandomly oriented short δ-alumina fibre-reinforced aluminium alloys has been investigated by instrumented impact testing. The impact toughness of these composites is shown to be pseudo-isotropic and extremely poor when compared with that of the unreinforced matrix alloys. This poor impact toughness is derived from the micromechanical mechanisms responsible for deformation which are dominated by the failure strain of the fibre reinforcement. This results in a low crack initiation energy and therefore a low impact toughness. This poor toughness is degraded further by a low crack propagation energy. It is concluded that the impact toughness of these MMC could be improved by the use of higher failure strain reinforcements, and/or by increasing the crack propagation energy by the introduction of additional energy absorbing mechanisms such as fibre pull-out.

1. Introduction

In recent years, metal matrix composites (MMC) have become the source of considerable scientific and industrial interest. These composite systems have exhibited improvements in modulus, and tensile and compressive strength similar to those shown in polymeric-based systems, and have also exhibited additional advantages over their polymeric competitors such as higher service temperatures and improved stability with respect to vacuum and ultraviolet radiation. MMC have also exhibited improvements in hot strength and modulus over the equivalent properties in the unreinforced matrix alloys. This latter behaviour, in particular, has stimulated considerable commercial interest in these materials. However, a common feature of ceramic fibre-reinforced MMC is low ductility and often poor toughness.

The correct approach for the evaluation of toughness in composites is still the subject of some debate. In systems where the crack initiation energy dominates the fracture event, evaluation of the fracture toughness appears to be appropriate and yields a toughness parameter (K_{IC}) which is a characteristic material property. However, in composites where a significant contribution of the toughness arises from localized plasticity, crack blunting, pull-out and fibre/matrix delamination, K_{IC} no longer represents a simple characteristic of the material, the measured fracture toughness depending on a number of variables including the specimen gauge-length and width [1–3]. In some composites these processes can be optimized so that they become the dominant energy absorbing processes. In such composites, fracture toughness measurements are not appropriate and toughness is usually characterized by measurements of the fracture energy. This property is notoriously difficult to relate quantitatively to more specific parameters such as K_{IC} or to measurements of impact energy conducted on different sized specimens; however, it does allow a quantitative comparison of the toughness of different composite materials.

Toughness measurements have been made using both approaches on a number of MMC systems including B/Al [4, 5], FP alumina/Al [4], SiC whisker and particulate-reinforced aluminium [6, 7] and C/Al [8]. Both approaches reveal that these systems usually have relatively poor toughness, with K_{IC} as low as $7\,\mathrm{MPa\,m^{1/2}}$ [4, 6, 7] and fracture energies between 10 and $75\,\mathrm{kJ\,m^{-2}}$ [4] depending on the type of reinforcement and its physical form. Transverse toughnesses are also low, with typical values at least one order of magnitude lower than the axial value [8].

The type of reinforcement plays a significant role in controlling toughness. Carbon-reinforced MMC are generally less tough than SiC or alumina composites [8], and boron-reinforced aluminium alloys are generally tougher but more susceptible to degradation of toughness in service than alumina-reinforced materials [4]. The morphology of the reinforcement is also important with particulate-reinforced materials generally exhibiting greater toughness than those reinforced with whiskers [6, 7]. These particulate-reinforced materials also exhibit a volume fraction dependence of toughness in contrast to whisker-reinforced materials, whose toughness is volume fraction independent [6].

Recently, a new type of ceramic short fibre has appeared which is composed predominantly of δ-alumina and which is characterized by good compatibility with aluminium alloys [9]. This short alumina fibre has been exploited in a number of applications where it has been used in a pseudorandom orientation to impart pseudo-isotropic improvements in high-temperature strength and modulus. Little, however, is known about the impact toughness of such short δ-alumina fibre-reinforced composites, particularly

0022–2461/88 \$03.00 + .12

TABLE I Alloy compositions and casting parameters

Alloy (wt %)	Die preheat (°C)	Preform preheat (°C)	Casting temp. (°C)	Duration of applied pressure (sec)
Al-4.0Zn-2.0Mg	520	520	1000	10
Al-12Si	515	515	950	10

where the fibre orientation is pseudorandom. This paper presents the results of an investigation into the impact response of such composites and the factors which control their toughness.

2. Experimental procedures

Composite material was prepared by a pressure infiltration technique [10] using preforms of pseudorandomly oriented short δ-alumina Saffil fibres (ICI trademark) and two aluminium alloy matrices. Table I contains the compositions of these alloys and the processing variables employed during casting of the materials. The densities of the preforms were in the range 0.66 to 0.71 $g\,cm^{-3}$ which produced a composite with a fibre volume fraction (V_f) of approximately 0.25. To allow comparison of the properties of the unreinforced alloys and composites, the volume of metal squeeze-cast was in excess of that required for infiltration of the preform. This made available both composite and unreinforced alloy processed under identical thermal/pressure conditions. Following each cast, the unreinforced alloy was machined from the composite producing two discs of 100 mm diameter and 15 mm thick. Round tensile specimens of 6 mm diameter and 30 mm gauge length were machined from these discs with their axes parallel to the plane of the disc, and these were tested using a conventional screw-driven tensile machine. Standard unnotched Charpy specimens were also machined from the discs with their long-axes parallel to the plane of the original preform.

The toughness of the composites was characterized by their dynamic fracture energy which was determined by instrumented impact testing of Charpy specimens. The instrumentation consisted of a transducer on the rear surface of the tup composed of four strain-gauges in a Wheatstone bridge arrangement. Following calibration, this transducer directly monitored the force on the tup during the fracture event, enabling the determination of the force/time relationship during fracture. These data were fed to a CEAST AFs/Mk2 transient recording system which provided digital measurements of force, energy, and displacement as well as graphical data such as force/time, energy/time and force/displacement. These allowed a detailed analysis of the fracture events in the materials.

Optical and scanning electron microscopy was employed to characterize the alumina-fibre preforms, the composite and alloy microstructures, and the fracture surfaces of the impact specimens.

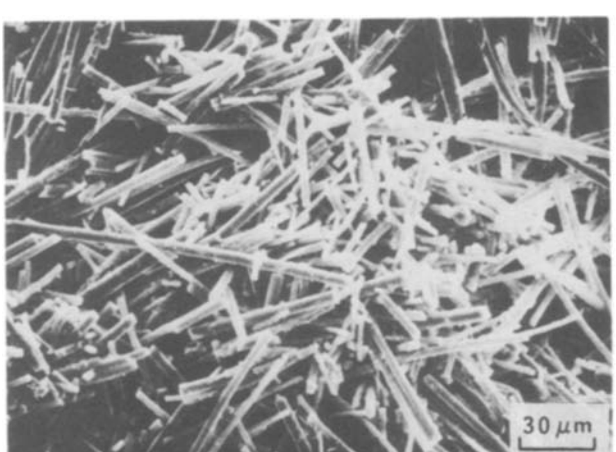

Figure 1 Scanning electron micrograph of an uninfiltrated Saffil preform.

3. Results

Fig. 1 shows a scanning electron micrograph of a typical uninfiltrated δ-alumina fibre preform which confirms the interlocked pseudo three-dimensional random nature of the preform, and therefore the resulting pseudo-random arrangement of the fibres in the cast composites. Fig. 2 shows typical microstructures of the cast composites with Al-4.0Zn-2.0Mg and Al-12Si matrices. All the composites were of good quality with little evidence of porosity or the ingress of dross or inclusions. The grain sizes in the matrices of the composites were generally smaller than those of the unreinforced alloys cast under the same conditions and in the case of the Al-Si matrix, the eutectic was generally finer and showed some signs of a divorced eutectic with preferential nucleation of silicon plates around the fibres.

Table II contains the average tensile data obtained from both the unreinforced matrix alloys and the $0.25V_f$ composites. The addition of $0.25V_f$ alumina fibre to the Al-Zn-Mg and Al-Si alloys resulted in little or no reinforcement of the room-temperature strength. In the Al-Zn-Mg matrix composite there was a 3% reduction in strength compared with the unreinforced alloy and in the Al-Si matrix composite a 15% improvement in strength. All the composites exhibited low ductilities compared with the unreinforced matrix alloys, 1.5% elongation in the $0.25V_f$ alumina fibre Al-Zn-Mg composite and less than 1% in the case of the brittle matrix composite of 0.25 V_f alumina fibre Al-Si.

Table III shows the dynamic fracture energies of these composites. In order to determine whether the angle of impact with respect to the original preform orientation was significant, a limited number of impact tests were conducted on conventionally notched Charpy specimens with notch orientations 0° and 90° to the plane of the original fibre preform (Fig. 3 schematically illustrates the orientations of these

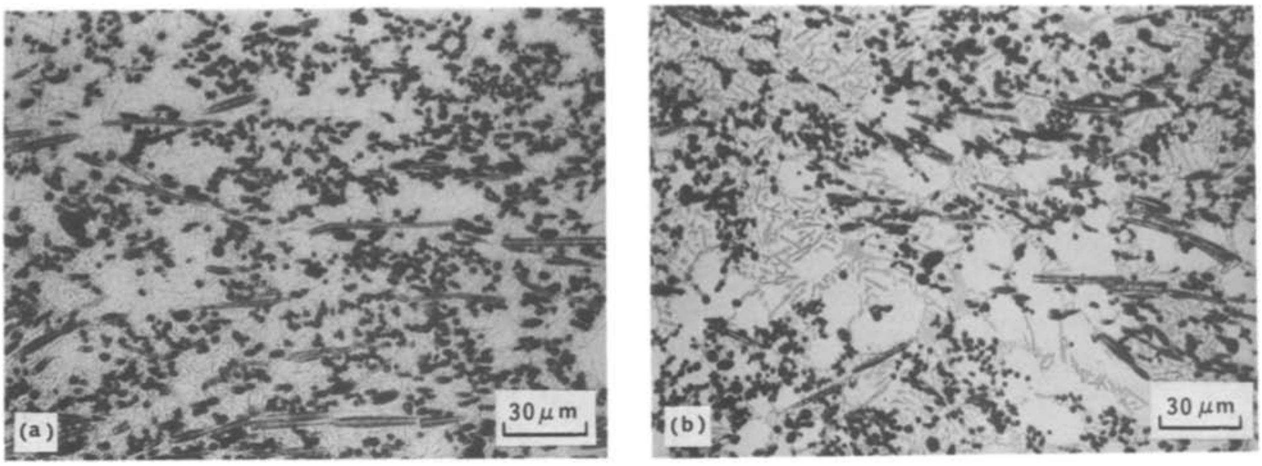

Figure 2 Optical micrographs of (a) $0.25V_f$ Saffil/Al–4.0Zn–2.0Mg, and (b) $0.25V_f$ Saffil/Al–12Si composites.

specimens). These tests were conducted on 0.25 V_f δ-alumina fibre/Al–Zn–Mg composites. The impact toughness from these tests were lower than those measured on unnotched specimens and average results are shown in Table III and are plotted in Fig. 4. There was only a marginal effect of impact orientation on the impact toughness of these composites.

Table III also contains the average fracture energies of Al–Zn–Mg and Al–Si alloys and composites measured on unnotched Charpy specimens. The fracture energy of Al–Zn–Mg composite was considerably lower than that of the unreinforced matrix alloy, the $0.25V_f$ composite having an impact toughness only 16% of the unreinforced matrix value. In the case of the more brittle Al–Si-based composites two responses were observed. The most common response was a lower impact toughness, approximately 65% of that of the brittle unreinforced alloy. However, in a minority of impact tests (on a single cast of material), the composite exhibited a significantly higher fracture energy, almost three times the value for the unreinforced matrix.

Fig. 5 shows typical instrumented impact data for these alloys and composites. Fig. 5a shows the force/time plot for unreinforced Al–Zn–Mg alloy. This response was typical of both matrix alloys and showed the development of force up to a maximum, equivalent to the dynamic ultimate tensile strength (UTS), at which point initiation of fracture occurred. This was then followed by a reduction in applied force as crack propagation proceeded. During the initiation stage the material showed an initially linearly elastic response followed by plastic deformation up to the dynamic UTS. Fig. 5b illustrates the comparable plot for a δ-alumina fibre-reinforced Al–Zn–Mg composite. The response of these composites was significantly different with a purely linear elastic response during the initiation of fracture, followed by rapid crack propagation. This significantly different response with a smaller area under the force/time curve (which is proportional to the force/displacement curve) confirmed the macroscopic fracture energy measurements, i.e. the composite exhibited lower impact toughness than the unreinforced matrix alloy as a result of its brittle response.

Figs 6 and 7 illustrate typical fractographs from the unreinforced alloys and composites. Fig. 6a shows the fracture surface of the Al–Zn–Mg alloy which was ductile in nature, consistent with the static tensile ductility of 11.5%. Fig. 6b shows the fracture surface of a $0.25V_f$ δ-alumina fibre-reinforced Al–Zn–Mg composite. This material showed a rather brittle response with simple fracture of the reinforcing fibres and little evidence of extensive matrix ductility. There was also no evidence of fibre pull-out.

Figs 7a and b show the fracture surface of the unreinforced Al–Si alloy. This fracture was brittle in nature with evidence of extensive cleavage fracture through the brittle plates of eutectic silicon. Figs 7c, d and e illustrate the fracture surfaces of the Al–Si composites which exhibited the two significantly different impact responses. Fig. 7c shows a typical fracture surface of a material which exhibited poorer impact toughness than the matrix alloy. These fracture surfaces revealed a response similar to that obtained from the Al–Zn–Mg-based composites with simple fibre fracture and a low ductility matrix response. However, in the material which exhibited improved impact

TABLE II Average tensile data for unreinforced and reinforced alloys

	UTS (MPa)	Elongation (%)	No. casts
Unreinforced Al–4.0Zn–2.0Mg	273	11.5	6
$0.25V_f$ Al–4.0Zn–2.0Mg	266	1.5	6
Unreinforced Al–12Si	143	7.0	4
$0.25V_f$ Al–12Si	165	< 1.0	4

TABLE III Average dynamic fracture energies for unreinforced and reinforced alloys

	Dynamic fracture energy ($kJ\,m^{-2}$)	
	Unnotched	Notched
Unreinforced Al–4.0Zn–2.0Mg	184	–
$0.25V_f$ Al–4.0Zn–2.0Mg	30	16* 15†
Unreinforced Al–12Si	35	–
$0.25V_f$ Al–12Si	23 95	–

Notch orientation relative to preform plane, *0° orientation, †90° orientation.

toughness, there was a significantly different fracture behaviour. Figs 7d and e show typical fractographs from this material. The matrix response was still low ductility in nature, but rather than exhibiting simple failure of the reinforcement at the fracture surface, the composite exhibited extensive fibre pull-out.

4. Discussion

Table III and Fig. 4 illustrate the nature of the impact response of these pseudorandomly oriented short δ-alumina fibre-reinforced aluminium alloys. Table III shows that most of these composites were considerably less tough than the unreinforced matrix alloys. This is consistent with the fractographs in Figs 6 and 7 which show extremely low ductility fracture surfaces. These pseudorandomly reinforced materials also exhibited this poor impact toughness pseudo-isotropically (Fig. 4). The important question which must, therefore, be answered is, why do these composites exhibit such extremely low fracture energies?

Some indication of the source of this low toughness can be seen from the force/time data in Fig. 5. It is clear from Figs 5a and b that these composites exhibited significantly different impact responses to the unreinforced matrix alloys, and the low energies absorbed during impact resulted from two sources. The first source of poor impact toughness was the lack of macroscopic plastic deformation prior to crack initiation. Fig. 5b shows the crack initiation and

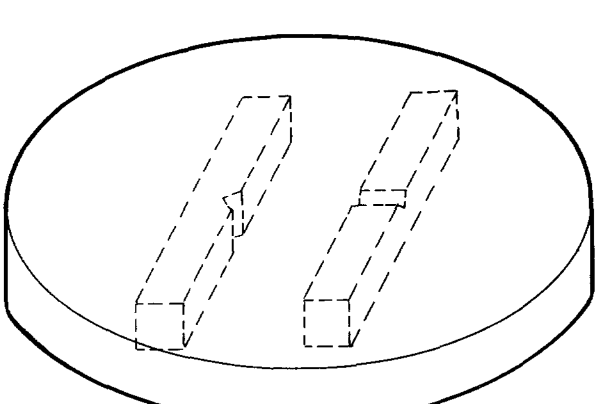

Figure 3 Orientation of the notched charpy specimens relative to the original preform.

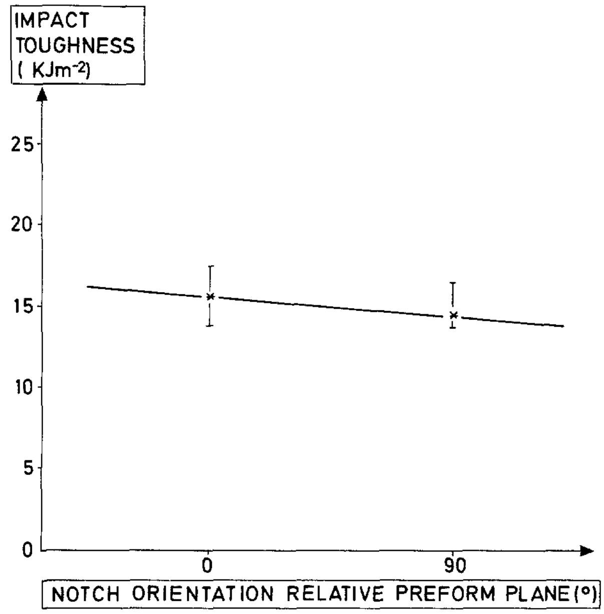

Figure 4 The effect of notch orientation on the impact toughness of a $0.25V_f$ Saffil/Al–4.0Zn–2.0Mg composite.

propagation behaviour during impact of a composite. The composite response during the initiation stage was purely elastic with the result that the energy absorbed during deformation was extremely low. The second source of poor toughness was the extremely small energy absorbed during crack propagation. The act of manufacturing the composites, therefore, appears to considerably alter the micromechanics of deformation such that both the crack initiation and propagation behaviour of the matrix alloys are significantly changed. It is therefore important to identify the micromechanical deformation mechanisms present during such fracture events.

The micromechanical mechanisms taking place during composite deformation can be analysed under static conditions using a rule of mixtures (ROM) analysis, and an earlier paper [11] has analysed this using a simple ROM formalism modified to account for the short fibre and its pseudorandom orientation. The data required for this type of analysis are the static tensile properties of the fibre reinforcement and unreinforced alloy, similar to those contained in Table II. The important problem to be resolved, however, is whether such an analysis, based on static strength, can be extended to analyse the behaviour in tests conducted under dynamical conditions. Some evaluation of the validity of this can be obtained by considering the static and dynamic strength differences between the unreinforced matrix alloys and their equivalent composites.

Fig. 8 shows the calculated ROM diagrams derived from this static analysis for composites based on Al–4.0Zn–2.0Mg and Al–12Si. It is clear that the fibre fractions in this work lie in the vicinity of, or below V_{crit}, the critical volume fraction of reinforcement required for composite strengths above that of the unreinforced matrix alloy. The composite strengths do not, therefore, differ significantly from the strength of the unreinforced matrix alloy (Table II). For example, in the case of the $0.25V_f$ δ-alumina fibre-

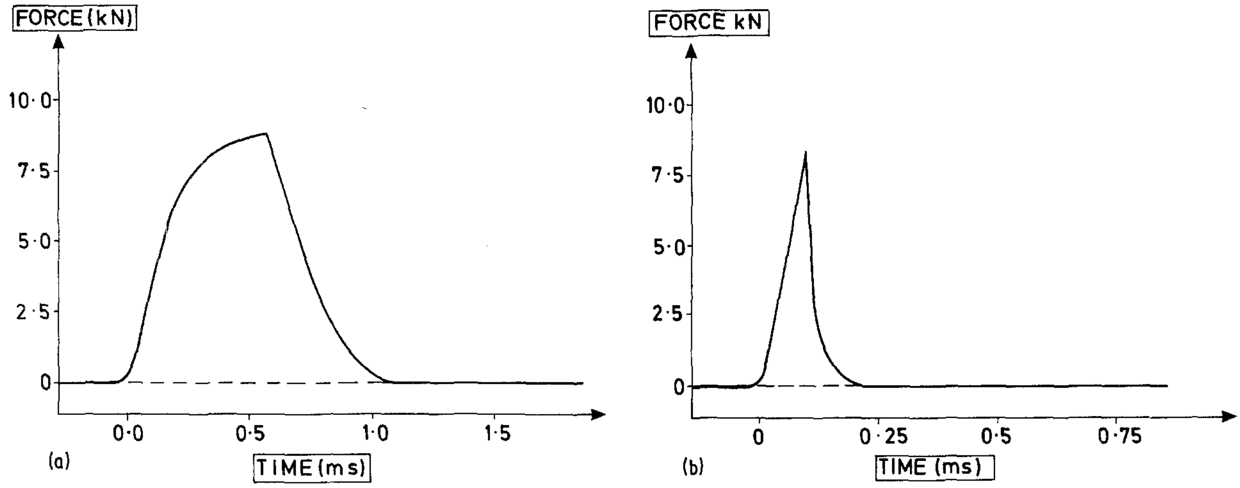

Figure 5 Force/time curves for (a) unreinforced Al–4.0Zn–2.0Mg, and (b) a $0.25V_f$ Saffil/Al–4.0Zn–2.0Mg composite.

reinforced Al–Zn–Mg composite the strength was 3% below that of the unreinforced matrix alloy. If one considers the data obtained under dynamical conditions, it is clear that a similar effect is observed.

If one considers the forces at crack initiation in Figs 5a and b (which are proportional to the dynamic UTS of the Al–Zn–Mg alloy and composite) it is clear that they are similar, with the composite exhibiting a maximum force 6% below that of the unreinforced matrix alloy. The difference in strength between the composite and matrix alloy measured statically and dynamically are therefore similar and within normal experimental scatter. It can therefore be concluded that the micromechanical mechanisms taking place during the initiation of fracture are qualitatively the same under both static and dynamical conditions. The static analysis of the micromechanical mechanisms present during deformation can, therefore, be extended to qualitatively describe the deformation under impact conditions.

Fig. 8 allows a qualitative description of the micromechanics of static deformation. The important parameter to assess this behaviour is V_{min}. At volume fractions less than V_{min} the composite deformation occurs by a multiple fibre fracture mechanism. In this case, the composite deformation behaviour contains a significant component derived from matrix deformation. However, above V_{min} fibre failure causes immediate catastrophic failure of the composite. In this case the composite deformation response is controlled predominantly by the characteristics of the fibre (in particular the fibre failure strain) and not by the matrix properties. If one identifies the position of these $0.25V_f$ composites on their appropriate ROM diagrams (Fig. 8) it is clear that the composites have $V_f > V_{min}$ and will therefore exhibit the latter response. In such cases the composite failure strains are controlled predominantly by the fibre properties which accounts for both the low composite failure strains and the low fracture energies.

The simple ROM micromechanical analysis, therefore, qualitatively accounts for (i) the poor composite impact toughness, and (ii) the significant difference between the fracture behaviour of the composites and unreinforced matrix alloys. However, this model also implies that the composite failure strains will be

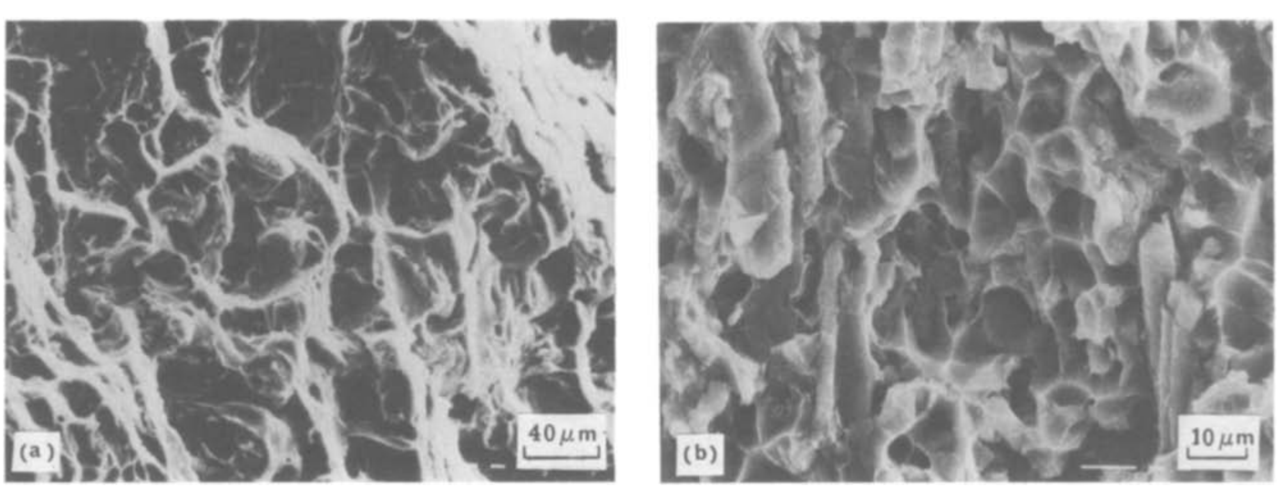

Figure 6 Fracture surfaces of (a) unreinforced Al–4.0Zn–2.0Mg, and (b) a $0.25V_f$ Saffil/Al–4.0Zn–2.0Mg composite.

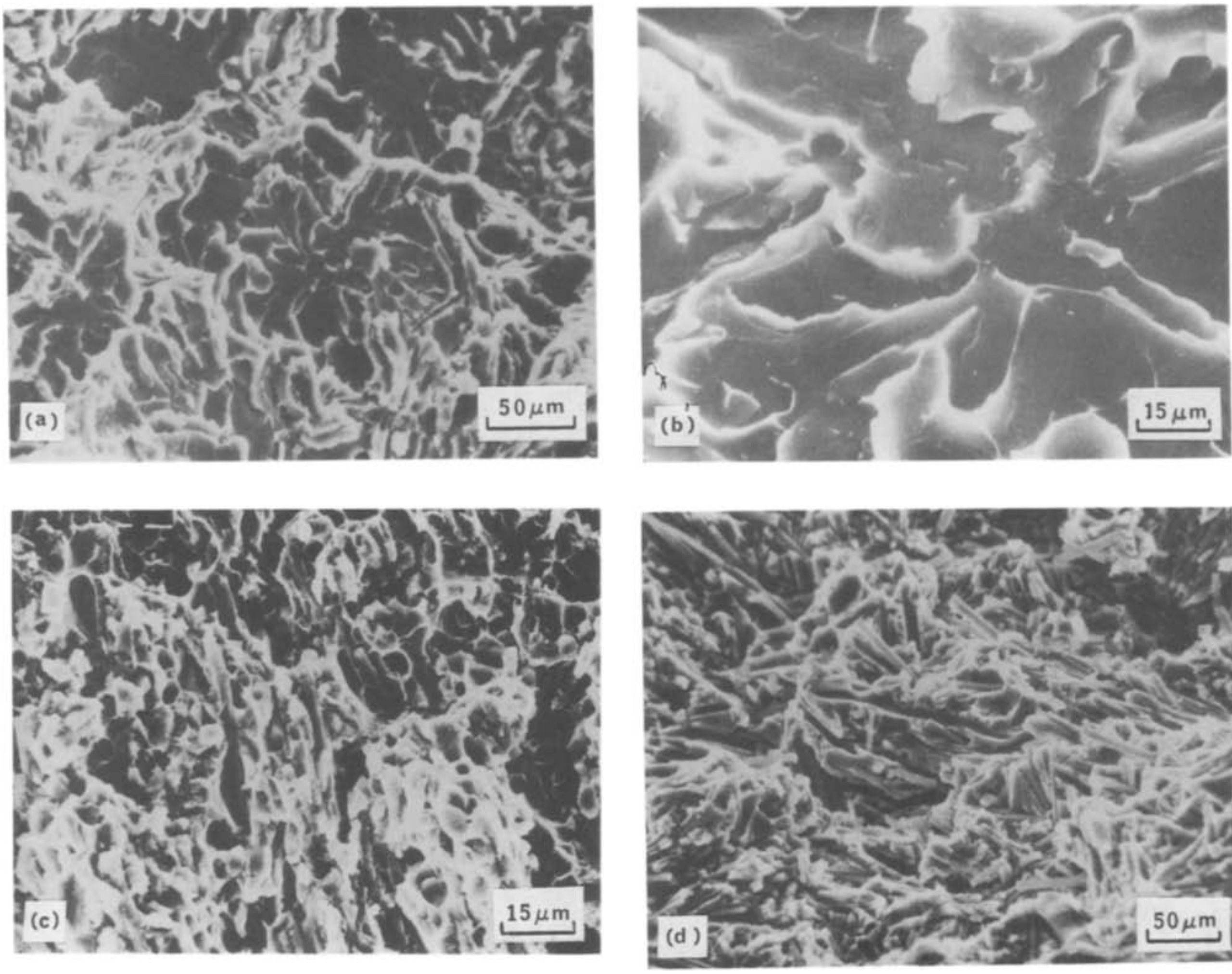

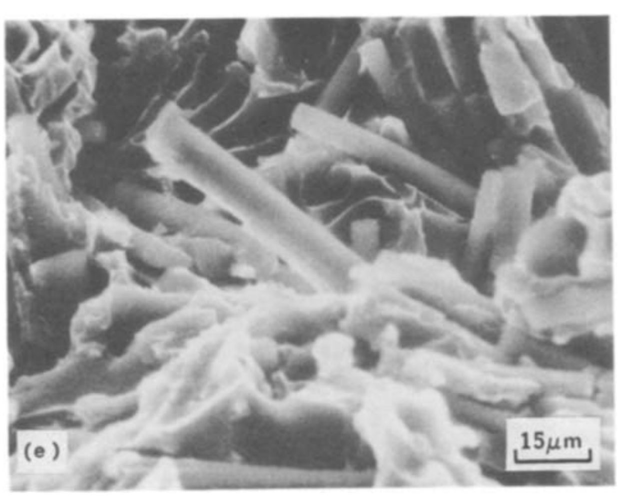

Figure 7 Fracture surfaces of (a), (b) unreinforced Al–12Si, (c) a low fracture energy 0.25 V_f Saffil/Al–12Si composite, and (d), (e) a high fracture energy 0.25V_f Saffil/Al–12Si composite.

identical and of the order of 0.67% (the failure strain of Saffil fibres). This is clearly an oversimplification and occurs because the simple ROM model assumes that all the fibres are loaded to the same fibre stress and fail at the same stress level. This is too simple a description for these composites, because (i) the pseudorandom orientation of the fibres results in a distribution of fibre stresses, and (ii) these ceramic fibres exhibit a statistical variation in fibre strength. In practice, the composite failure strains will therefore not be identical. Variation in composite failure strain will arise because of the presence of unfractured fibres bridging the developing fracture surface. Strains above the failure strain of the reinforcement must, therefore, be applied to fully fracture the composite, and this higher strain will be partially accommodated by localized matrix deformation. This then accounts for the composite failure strains above 0.67%, and is the reason for the larger composite failure strains observed in more ductile matrix composites. The simple model is useful, however, in qualitatively analysing the reasons for the low fracture energies in these MMC and how improved toughness could be developed.

The static and dynamic behaviour of these composites is controlled predominantly by the fibre failure strain which accounts for both the low composite failure strain and the low crack initiation energy. This implies that all ceramic fibre-reinforced MMC will exhibit low dynamic fracture energies due to the small failure strain of the reinforcement. There are, therefore, two possible solutions to improve toughness in MMC:

1. increase the failure strain of the reinforcement to increase the initiation energy for fracture, and/or
2. increase the propagation energy during fracture by adding extra energy absorbing mechanisms.

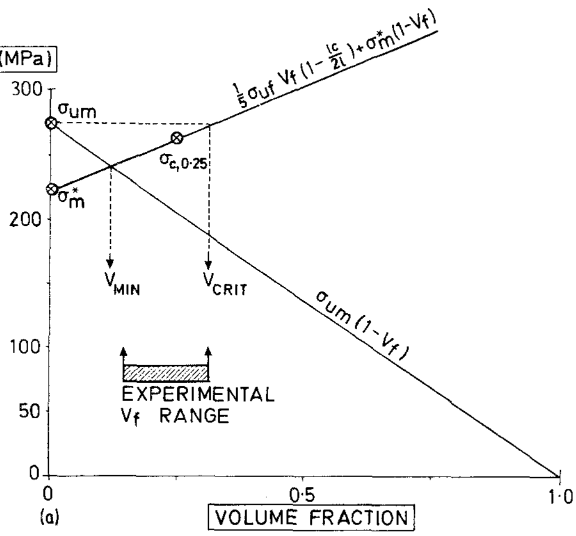

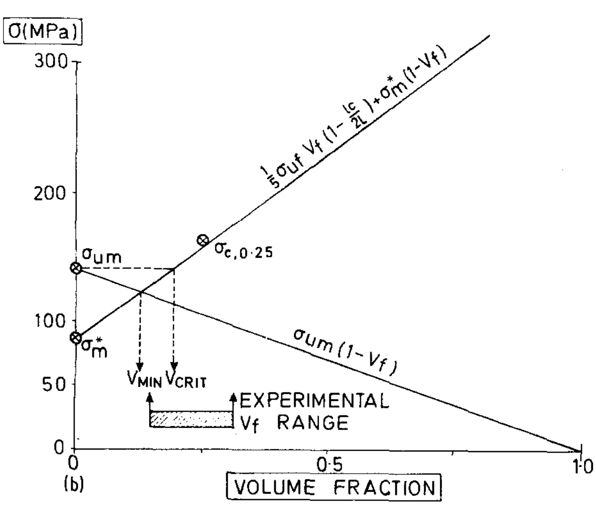

Figure 8 ROM strength prediction for Saffil-reinforced (a) Al–4.0Zn–2.0Mg, and (b) Al–12Si.

4.1. Increasing the reinforcement failure strain

As the impact toughness of these composites appears to be controlled by the fibre failure strain, their toughness should be improved by the use of a reinforcement with a higher failure strain. This is clearly impossible with ceramic fibres, because all these materials exhibit maximum failure strains of approximately 1%; however, if high strength metallic reinforcements are employed the ductility of the metal wires could be exploited to increase the composite failure strain. In such cases the dynamic UTS of the composite will generally be lower than that obtained with ceramic reinforcement but the increased strain to failure will balance this reduction in UTS to produce improved toughness. This is shown schematically in Fig. 9a, and Fig. 9b shows an instrumented impact force/time curve for a $0.21 V_f$ steel wire-reinforced Al–4.0Zn–2.0Mg composite. This composite exhibited extremely good impact toughness due, in part, to the increased initiation energy resulting from the improved composite failure strain.

4.2. Increasing the crack propagation energy

The alternative route to tougher MMC appears to be via control of the crack propagation energy. This is already well exploited in polymeric-based composites (in particular those with brittle reinforcements and matrices). In such composites the crack propagation energy is usually the dominant source of composite toughness through processes such as fibre pull-out and fibre/matrix debonding. The role of these processes in δ-alumina fibre-reinforced aluminium alloys is uncertain at present, because most composites containing δ-alumina fibres do not exhibit pull-out. Table IV summarizes the results of simple model calculations [12] for the pull-out, debond and fracture strain energy components of δ-alumina/Al–4.0Zn–0.2Mg and Al–12Si composites. It is clear that the contributions due to these processes are small. The propagation energy

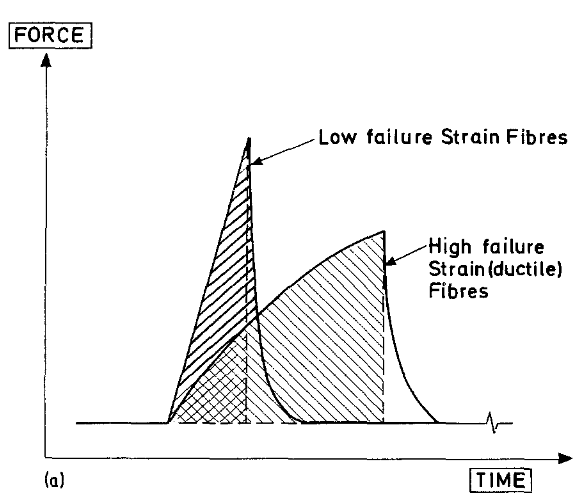

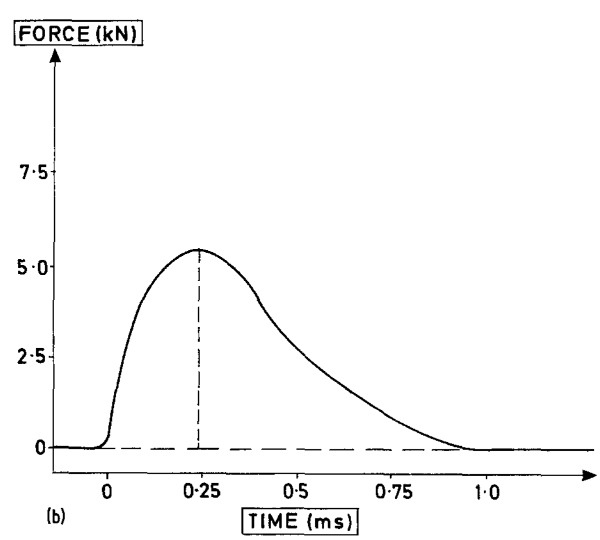

Figure 9 (a) Schematic force/time curves for composites containing low and high failure-strain reinforcements. (b) Force/time curve for a $0.21 V_f$ steel wire-reinforced Al–4.0Zn–2.0Mg composite.

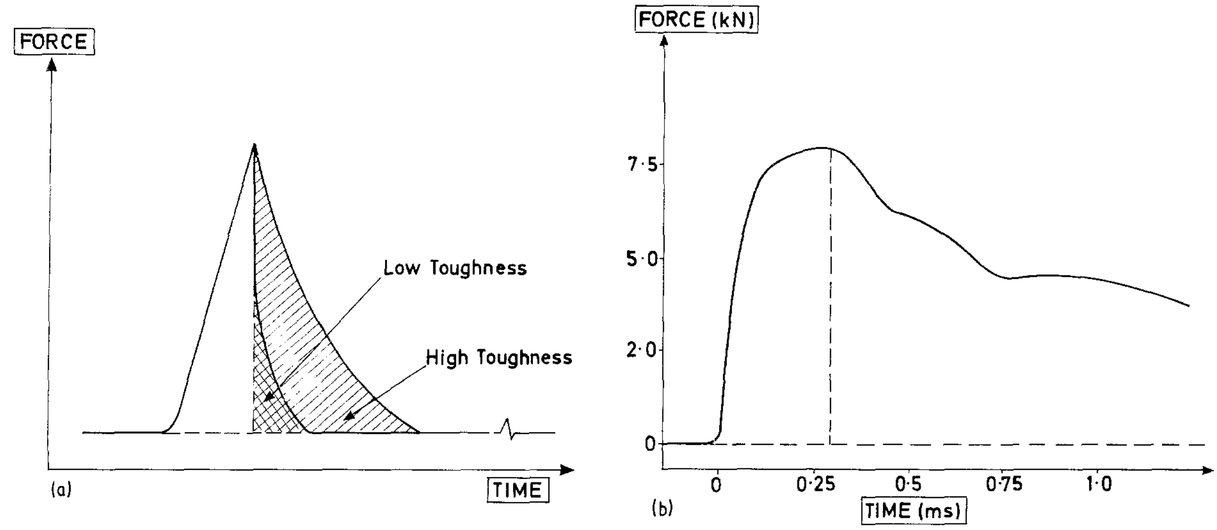

Figure 10 (a) Schematic force/time curves for composites exhibiting low and high crack propagation energies. (b) Force/time curve for a steel wire-reinforced Al–4.0Zn–2.0Mg composite.

is, therefore, mainly controlled by the matrix alloy's fracture energy which is relatively small due to the cohibitive effect of the fibre array [12]. An investigation of the propagational processes in these composites could, however, lead to improvements in their impact toughness. Fig. 10a schematically illustrates how improved impact toughness could be obtained by this route and Fig. 10b shows the impact response of an MMC where the propagational processes contributed extensively to the dynamic fracture energy. In these steel wire/Al–Zn–Mg composites the primary source of this improved toughness was pull-out of the reinforcement which resulted from (i) a poor interfacial bond and therefore a large critical fibre length, and (ii) a large diameter reinforcement. This system is rather different from δ-alumina fibre-reinforced alloys, but illustrates a case where the propagational processes can be optimized to produce extensive energy absorption. The problem with δ-alumina-reinforced composites is shown in Table IV. The fibres are very fine and bond extremely well to aluminium matrices generating a high interfacial shear strength, and a small critical fibre length. These factors usually combine to produce little debonding or pull-out and result in low propagation energies. However, in certain cases, significant amounts of these processes can be induced. Figs 7d and e illustrate this in a δ-alumina/Al–12Si composite. In these composites the pull-out events were clearly associated with a higher fracture energy. The precise causes of this pull-out are uncertain at present; however, the presence of pull-out indicates that a systematic investigation of the role of interfacial bond on the impact toughness in δ-alumina fibre-reinforced aluminium alloys could provide a route to the development of tougher MMC. Such studies should investigate the effect of interfacial bond strength on toughness by systematic control of factors such as (i) surface pretreatment of the fibres, (ii) matrix alloy chemistry (in particular the role of magnesium content [13]), and (iii) the processing route.

TABLE IV Pull-out, debonding and fibre fracture strain contributions to the propagation energy of $0.25 V_f$ δ-alumina-reinforced composites

Matrix alloy	Propagation energy contribution ($kJ\,m^{-2}$)		
	Pull-out (max)	Debonding (max)	Fibre fracture strain (max)
Al–4.0Zn–2.0Mg	0.9	0.2–1.6	0.05
Al–12Si	1.8	0.2–1.6	0.02

5. Conclusions

The impact toughness of pseudorandomly oriented short δ-alumina fibre-reinforced aluminium alloys is pseudo-isotropic and extremely poor when compared with that of the unreinforced matrix alloys.

This poor impact toughness derives from (i) a low initiation energy for fracture as a result of the low composite failure strain, and (ii) a low crack propagation energy. It should, therefore, be possible to improve the impact toughness of these MMC by (a) the use of higher failure strain reinforcements such as metallic filaments or wires, and/or by (b) increasing the crack propagation energy by the introduction of additional energy absorbing mechanisms such as pull-out and fibre/matrix debond, produced by controlling the strength of the fibre/matrix interface, and the aspect ratio of the reinforcement.

Acknowledgements

We thank Professor J. A. Belk for allowing the use of the experimental data in Figs 9 and 10, J. Bradfield and J. Crocker for experimental assistance, J. Dinwoodie, ICI (MOND Div.), for the supply of Saffil preforms, and J. Barlow, GKN Technology, for the notched composites.

References

1. K. G. KREIDER and L. DARDI, "Failure Modes in Composites I" (AIME, 1973) pp. 193–230.

2. P. W. M. PETERS, "Advances in Composite Materials", Proceedings ICCM 3, Vol. 2, Paris, August, 1980 (Pergamon, Oxford, 1980) pp. 1153–64.
3. M. A. WRIGHT, D. WELCH and J. JOLLAY, *J. Mater. Sci.* **14** (1979) 1218.
4. A. SKINNER, M. J. KOCZAK and A. LAWLEY, *Met. Trans.* **13A** (1982) 289.
5. D. WELCH and M. A. WRIGHT, *Fibre Sci. Technol.* **11** (1978) 447.
6. C. R. CROWE and R. A. GRAY, Proceedings, Failure Mechanisms in High Performance Materials, Gaithesbury, Maryland, USA, 1985 (Cambridge University Press, New York, 1985) pp. 157–66.
7. D. F. HASSON and C. R. CROWE, "Strength of Metals and Alloys", (ICSMA7) (Pergamon, Oxford, 1985) pp. 1515–20.
8. D. WEBSTER, "Advances in Composite Materials", Proceedings ICCM3, Vol. 2, Paris, August 1980 (Pergamon, Oxford, 1980) pp. 1165–76.
9. J. DINWOODIE, E. MOORE, C. A. J. LANGMAN and W. R. SYMES, Proceedings International Conference on Composite Materials, San Diego, California, July 1985.
10. T. W. CLYNE, M. G. BADER, G. R. CAPPELMAN and P. A. HUBERT, *J. Mater. Sci.* **20** (1985) 85.
11. C. M. FRIEND, *ibid.* **22** (1987) 3005.
12. M. R. PIGGOT, "Load Bearing Fibre Composites", 1st Edn (Pergamon, Oxford, 1980) pp. 126–40.
13. W. J. CLEGG, I. HORSFALL, J. G. MASON and L. EDWARDS, *Acta Metall.* in press.

Received 16 February
and accepted 23 June 1987